

## Conductivity distribution of resistor-capacitor composites

M. S. Choi and W. S. Kim

*Department of Physics, Pohang University of Science and Technology, P. O. Box 125, Pohang 790-600, South Korea*

Sung-Ik Lee

*Department of Physics, Pohang University of Science and Technology, P. O. Box 125, Pohang 790-600, South Korea  
and Physics Division, Research Institute of Industrial Science and Technology, Pohang, South Korea*

(Received 23 December 1993)

Conductivities of the  $N \times N$  percolation systems with resistors and capacitors mixed near the percolation threshold  $p_c$  were calculated. The statistical distribution of these conductivities were obtained after more than  $10^4$  configurations considered. We have shown that the argument of Rammal *et al.*, which is only for the case of dc response, can be properly extended to the case of nonzero capacitances (ac response). Some other interesting features, including the functional form, of the distribution were discussed as a function of the ratio  $\omega/\omega_0$  with  $\omega_0 \equiv 1/RC$ .

### I. INTRODUCTION

In a percolation system near the percolation threshold  $p_c$ , the percolation cluster forms a fractal;<sup>1,2</sup> hence on a length scale less than the correlation length, the local fluctuations of physical quantities are serious. Furthermore, the responses of such a system are affected by the local fluctuations, especially, by that of the ac conductivity  $\sigma(\mathbf{x}, \omega)$ , or equivalently the complex dielectric constant  $\epsilon(\mathbf{r}, \omega)$  in the system. Thus, the distribution of the macroscopic conductivity  $\Sigma$  of a percolation system is very important in understanding the physical properties of the system. In spite of its importance, however, little study of the conductivity distribution has been done.

For the dc case, where the admittances for the insulating bonds vanish, Rammal, Lemieux, and Tremblay obtained distribution by a computer simulation.<sup>3</sup> In their simulation, they found that the distribution is a function

of a single variable  $\Sigma/\Sigma_{av}$  (in this case,  $\Sigma$  and  $\Sigma_{av}$  are real) and that its relative width  $\Delta\Sigma/\Sigma_{av}$  is independent of geometrical details. Our result in this limiting case is consistent with theirs.

For the ac conductivity distribution of a percolation system near  $p_c$ , we present here another computer simulation using the transfer-matrix method. For this calculation, we assumed nonzero admittances of  $i\omega C$  for insulating (nonoccupied) bonds and the typical admittances  $1/R$  for the metallic (occupied) bonds. For simplicity, we introduced  $\omega_0$  defined as  $\omega_0 \equiv 1/RC$ . Then the distribution of the complex conductivity  $\Sigma$  was analyzed by its contour map on a complex conductivity plane while changing the ratio  $\omega/\omega_0 \equiv \omega'$ .

The importance of the ac conductivity distribution was emphasized recently when experimental results for the optical response of the metal-insulator composite were explained.<sup>4-6</sup> The theoretical calculation by Yagil and co-workers of the optical response was sensitive to the distribution of the ac conductivity. In their scaling theoretic study they conjectured a direct extension of the results

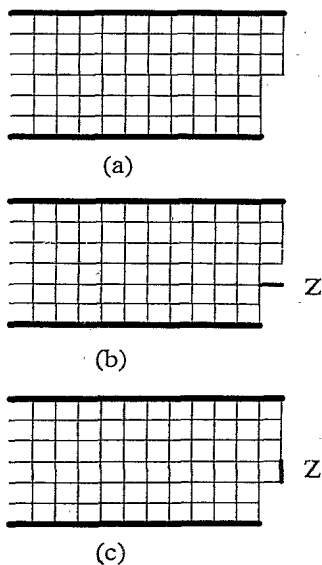


FIG. 1. The strip is constructed bond by bond. Each time we add a new impedance ( $Z$  or  $Z'$ ), the matrix  $A$  is modified (to  $A'$  or  $A''$ ) (see Ref. 8).

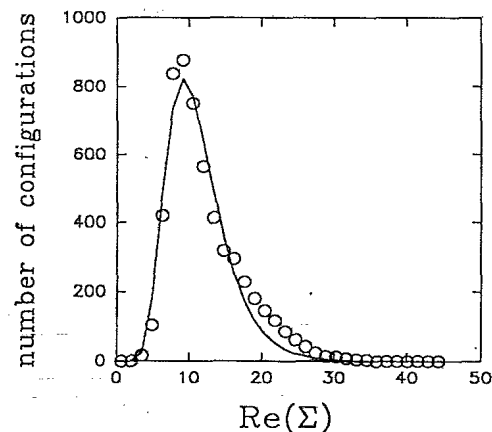


FIG. 2. The conductivity distribution in the limiting case  $C=0$ , along the real axis for the percolative peak. The solid line is a log-normal distribution function fitted with  $\text{Re}(\Sigma_{av})=9.23$  and  $\eta_x=0.44$ .

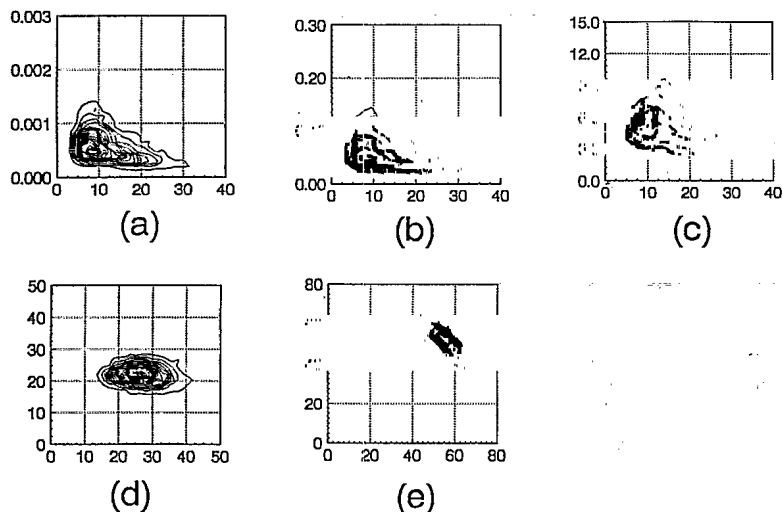


FIG. 3. Contour maps for the conductivity distribution of the  $10 \times 10$  system as the frequency  $\omega'$  increases. (a)  $\omega' = 10^{-6}$  (b)  $\omega' = 10^{-4}$  (c)  $\omega' = 10^{-2}$  (d)  $\omega' = 10^{-1}$  (e)  $\omega' = 10^0$ . The horizontal and vertical axes are those of  $\text{Re}(\Sigma)$  and  $\text{Im}(\Sigma)$ , respectively.

Rammal, Lemieux, and Tremblay to the ac case.<sup>7</sup> They assumed that, near  $p_c$ , the conductivity distribution is a function of the single variable  $\Sigma/\Sigma_{av}$  with its relative width independent of the frequency. From our simulation, however, we found that the ac conductivity distribution does not follow this conjecture.

In the next section, we present a simulation method we used to calculate the ac conductivity. In Sec. III, we give our results including a quantitative analysis of the distribution functions.

## II. SIMULATION METHOD

We used the transfer-matrix algorithm to calculate the conductivity of each percolation square of  $N \times N$ . This algorithm, which was developed by Derrida and co-workers to calculate the  $t$  exponent of a metal-insulator composite,<sup>8,9</sup> was further developed for the  $s$  exponent of a metal-superconductor composite.<sup>10</sup> This method can be applied even to a percolation system with insulating bonds of nonvanishing admittances.<sup>11,12</sup>

In the transfer-matrix algorithm, the admittance matrix  $A$  is introduced, whose elements  $A_{ij}$  are updated to  $A'_{ij}$  and  $A''_{ij}$  when a horizontal and a vertical bond, respectively, are inserted. Here we just give the formalism of the method:

$$A'_{ij} = A_{ij} - \frac{A_{i\alpha} A_{\alpha j} Z}{1 + A_{\alpha\alpha} Z}, \quad (1)$$

$$A''_{ij} = A'_{ij} + \frac{(\delta_{\alpha j} - \delta_{\beta j})(\delta_{\alpha i} - \delta_{\beta i})}{Z'}, \quad (2)$$

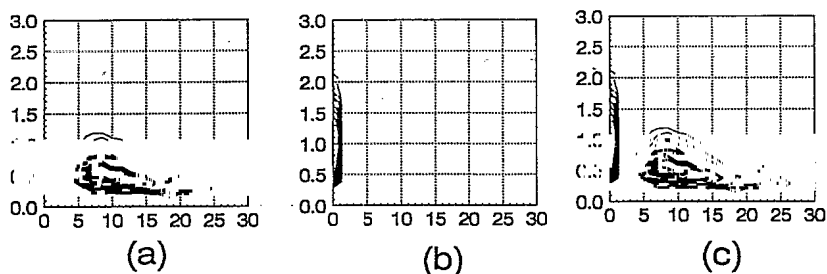


FIG. 4. The separate observations of distribution for the  $10 \times 10$  system: (a) the collection of percolative lattices, (b) the collection of nonpercolative lattices, (c) the overall. The horizontal and vertical axes are those of  $\text{Re}(\Sigma)$  and  $\text{Im}(\Sigma)$ , respectively.

where  $Z$  and  $Z'$  are the impedances of the inserted bond (Fig. 1).

## III. RESULT

Bond percolation systems of size  $N \times N$  for  $N = 5, 10$ , and 15 were considered. The probability  $p$  of the metallic occupation was chosen to be the percolation threshold  $p_c = 0.5$ . As mentioned above, we assigned the admittance  $1/R$  once a bond is occupied, but  $i\omega C$  if it is not occupied. For the statistical analysis, we generated more than  $10^4$  configurations for each  $N$  and  $\omega' \equiv \omega/\omega_0$ . We used the contour maps to display the general behavior of the conductivity distribution.

For the validity test of our simulation, we show the histogram for  $\omega' = 0$  in Fig. 2. We found that the distribution fits a log-normal distribution function (see the Appendix) of the single variable  $\Sigma/\Sigma_{av}$  and that, as observed by Rammal, Lemieux, and Tremblay, the relative width  $\Delta\Sigma/\Sigma_{av}$  is independent of the size  $N$ .

After investigating the behavior of the conductivity distribution as a function of the frequency ( $\omega'$ ), we found several interesting features. The main features of our calculations are as follows (Fig. 3): (a) Two peaks in the distribution merge and then separate again as  $\omega'$  increases. (b) As  $\omega'$  increases, the shape of the distribution rotates. (c) The distribution for the frequency  $\omega'$  is similar to the reflected image of that for the frequency  $1/\omega'$  against the ray  $\Sigma = r \exp[i\pi/4]$ ,  $0 < r < \infty$ . (d) For  $\omega' \ll 10^{-1}$ , the distribution fits a log-normal distribution function, but elsewhere it cannot be fitted to any simple analytic function.

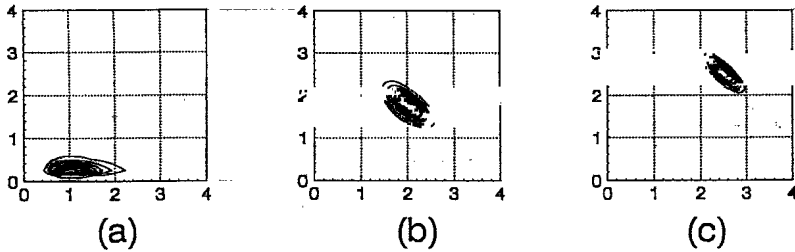


FIG. 5. Contour maps of the two-dimensional log-normal distribution function. (a)  $\eta_x = \eta_y = 0.45$  (b)  $\eta_x = \eta_y = 0.20$  (c)  $\eta_x = \eta_y = 0.12$ . The horizontal and vertical axes are those of  $\text{Re}(\Sigma)$  and  $\text{Im}(\Sigma)$ , respectively.

We discuss the details of the conductivity distribution in the two typical regions:  $\omega' \ll 10^{-1}$  and  $\omega' \approx 1$ . The high-frequency limit is simply guessed from the low-frequency limit by means of the symmetry argument. Furthermore, for convenience of discussion, we classify each configuration in the ensemble into the percolative or the nonpercolative lattice according to whether it has a percolating cluster or not.

#### A. Low-frequency region ( $\omega' \ll 10^{-1}$ )

In this region, the origin and the merging behavior of the two peaks can be understood in a simple way. First, the two peaks originate from the percolative and the nonpercolative lattices, respectively. This is confirmed by considering the distribution of the percolative and the nonpercolative lattices separately. Each peak in the separate distributions is identical to the corresponding one in the original overall distribution (Fig. 4), so that the merging of the two peaks as increasing  $\omega'$  is straightforward. As  $\omega'$  increases from the low capacitive coupling region, the imaginary part of the total admittance for the percolative lattice increases and the percolative peak moves to the point on the ray  $\Sigma = r \exp[i\pi/4]$ ,  $0 < r < \infty$ . For the nonpercolative lattices, the real part of the admittances increase under the influence of the increasing  $i\omega C$ . Once the magnitude of  $i\omega C$  is comparable with that of  $1/R$ , the real and imaginary part of the two peaks should be in the same region, and the two peaks merge into one.

Furthermore, the distribution fits quite well a two-dimensional log-normal distribution function (Fig. 5):

$$P(x,y) \propto \exp \left[ -\frac{1}{2} \frac{\ln^2(x/a_x)}{s_x^2} \right] \times \exp \left[ -\frac{1}{2} \frac{\ln^2(y/a_y)}{s_y^2} \right], \quad (3)$$

where

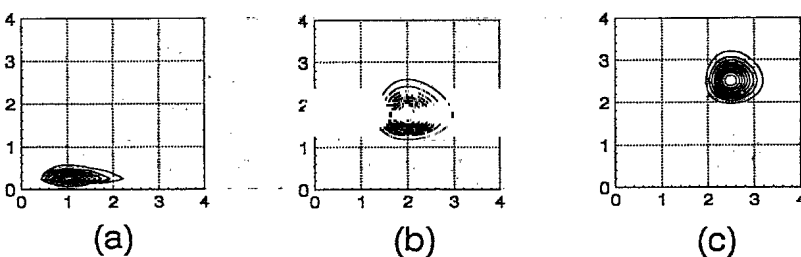


FIG. 6. Contour maps of the modified log-normal distribution function. (a)  $\eta_x = \eta_y = 0.45$ ;  $\gamma_x = \gamma_y = 10^6$  (b)  $\eta_x = \eta_y = 0.20$ ;  $\gamma_x = \gamma_y = 0.250$  (c)  $\eta_x = \eta_y = 0.12$ ;  $\gamma_x = \gamma_y = 0.150$ . The horizontal and vertical axes are those of  $\text{Re}(\Sigma)$  and  $\text{Im}(\Sigma)$ , respectively.

$$\Sigma = x + iy, \quad (4)$$

$$\Sigma_{av} = a_x + ia_y, \quad (5)$$

$$s_x = 1 + \eta_x, \quad (6)$$

$$s_y = 1 + \eta_y. \quad (7)$$

From the calculation we obtained the relative width of  $\eta_x = \eta_y = 0.45$  for both the percolative and the nonpercolative peaks.

#### B. The region $\omega' \approx 1$

In this region, the distribution function (3), which is good for  $\omega' \ll 10^{-1}$ , is not satisfactory. The shape of the distribution rotates smoothly with increasing  $\omega'$ . Furthermore, the relative widths  $\eta_x$  and  $\eta_y$  are much reduced. The deviation of the distribution function near  $\omega' \approx 1$  motivates us to modify the distribution function introducing another characteristic parameter  $\gamma$ :

$$P(x,y) \propto \exp \left[ -\frac{1}{2} \frac{\ln^2(x/a_x)}{s_x^2} \right] \times \exp \left[ -\frac{1}{2} \frac{\ln^2(y/b_y)}{s_y^2} \right] \times \exp \left[ -\frac{1}{2} \left[ \frac{(x-a_x)}{\gamma_x} + \frac{(y-a_y)}{\gamma_y} \right]^2 \right]. \quad (8)$$

This simple modification at the third exponential factor describes the rotation of the distribution quite well (Fig. 6). In this frequency range, the values of the parameters  $\eta_x$ ,  $\eta_y$ ,  $\gamma_x$ , and  $\gamma_y$  depend strongly on the frequency (Fig. 7). Note that, outside this region, the values of the parameters  $\gamma$  are so large that the modification is not needed.

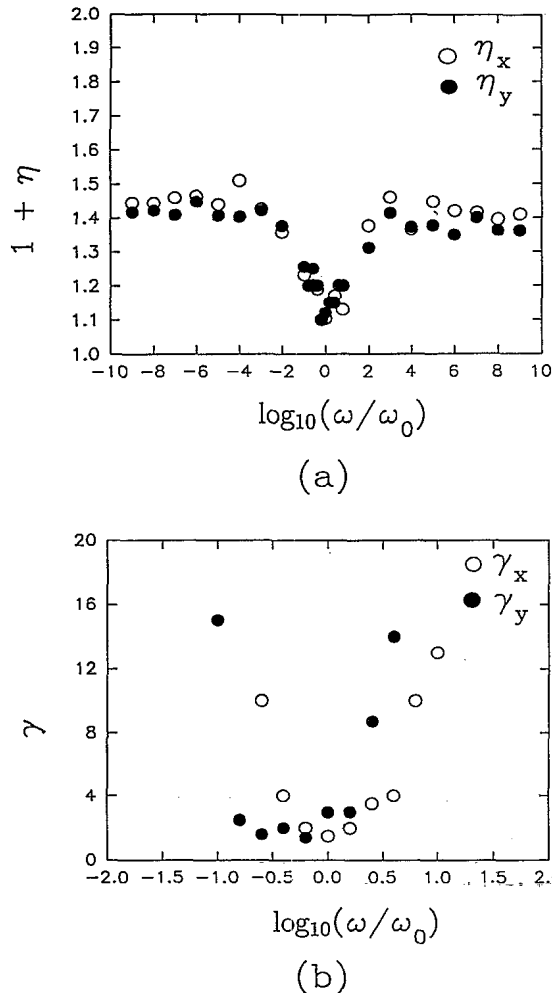


FIG. 7. (a) the relative width  $\eta$  and (b) the correction parameter  $\gamma$  as a function of frequency  $\omega'$ .

#### IV. CONCLUSION

We have calculated the conductivity in a  $N \times N$  lattice consisting of metal and capacitor near the percolation threshold, and extensively studied the argument of Rammal, Lemieux, and Tremblay, originally suggested only for the metal-insulator system. After calculating more than  $10^4$  configurations for each  $N$  and  $\omega'$ , we present a conjecture about the conductivity distribution, which is

just a more careful extension of the argument of Rammal, Lemieux, and Tremblay (or a modification of the conjecture of Yagil and co-workers): *the distribution is a function of  $Re(\Sigma)/Re(\Sigma_{av})$ ,  $Im(\Sigma)/Im(\Sigma_{av})$  and the ratio  $\omega' \equiv \omega/\omega_0$ , but independent of the geometric details such as the size  $N$  or the type of the lattice (although we have investigated only the square lattice). The frequency ( $\omega'$ ) dependence of the distribution was investigated through the relative widths  $\eta$  and the correction parameters  $\gamma$ .*

#### APPENDIX

The log-normal distribution for a random variable  $x$  is given by the following equations:

$$f(x) = \frac{1}{\sqrt{2\pi s} a e^{(1/2)s^2}} \exp\left[-\frac{1}{2} \frac{\ln^2(x/a)}{s^2}\right],$$

$$s = \ln(1 + \eta), \quad 0 \leq \eta < 1.$$

The peak position is specified by the parameter  $a$ . The parameter  $s$  or, more conveniently, the parameter  $\eta$  specifies the relative width of the distribution.

We summarize the statistics of the variable  $x$  on the log-normal distribution function:

$$x_R = a(1 + \eta),$$

$$x_L = \frac{a}{1 + \eta} \sim a(1 - \eta),$$

$$\langle x \rangle = a e^{(3/2)s^2},$$

$$\langle x^2 \rangle = a^2 e^{4s^2},$$

$$\langle (\Delta x)^2 \rangle = a^2 e^{3s^2} \sqrt{e^{s^2} - 1},$$

$$\frac{\sqrt{\langle (\Delta x)^2 \rangle}}{\langle x \rangle} = \sqrt{e^{s^2} - 1} \sim \eta,$$

where  $x_R$  and  $x_L$  are the right and the left limit of  $x$  which has an appreciable probability.

#### ACKNOWLEDGMENTS

The authors are grateful for very helpful discussion with Sung Ho Salk. This work was supported by the Korean Ministry of Education through the Korea Research Foundation and by the Foundation of Science and Technology through the Advanced Material Research Center.

<sup>1</sup>Jens Feder, *Fractals* (Plenum, New York, 1988).

<sup>2</sup>D. Stauffer, *Introduction to Percolation Theory* (Taylor and Francis, London, 1985).

<sup>3</sup>R. Rammal, M. A. Lemieux, and A. M. S. Tremblay, *Phys. Rev. Lett.* **54**, 1087 (1985).

<sup>4</sup>P. Gadenne, Y. Yagil, and G. Deutscher, *Physica A* **157**, 279 (1989).

<sup>5</sup>P. Gadenne, Y. Yagil, and G. Deutscher, *J. Appl. Phys.* **66**(7), 3019 (1989).

<sup>6</sup>Y. Yagil and G. Deutscher, *Appl. Phys. Lett.* **52**(5), 373 (1988).

<sup>7</sup>Y. Yagil, M. Yosefin, D. J. Bergman, and G. Deutscher, *Phys. Rev. B* **43**, 11 343 (1991).

<sup>8</sup>B. Derrida, J. G. Zabolitzky, J. Vannimenus, and D. Stauffer, *J. Stat. Phys.* **36**, 31 (1984).

<sup>9</sup>B. Derrida and J. Vannimenus, *J. Phys. A* **15**, L557 (1982).

<sup>10</sup>H. J. Herrmann and B. Derrida, *Phys. Rev. B* **30**, 4080 (1984).

<sup>11</sup>A. L. Bug, G. S. Grest, M. H. Cohen, and I. Webman, *J. Phys. A* **19**, L323 (1986).

<sup>12</sup>J. M. Laugier, J. Clerc, G. Giraud, and J. M. Luck, *J. Phys. A* **19**, 3153 (1986).